Electronic Supplementary Information for

Synthesis and properties of furan-based imine-linked porous organic frameworks

Jiping Ma, Min Wang, Zhongtian Du, Chen Chen, Jin Gao and Jie Xu*

Dalian National Laboratory for Clean Energy, State Key Laboratory of Catalysis, Dalian Institute of Chemical Physics, Chinese Academy of Sciences, Dalian, 116023, P. R. China

*Corresponding author: E-mail: **xujie@dicp.ac.cn**

Content:

1. Materials

m-Phenylenediamine (98%), benzidine (95%) and 2,6-diaminopyridine (98%) were purchased from Aladdin Chemistry Co. Ltd. *p*-Phenylenediamine (99%) was from J & K Scientific Ltd. Activated carbon (coconut shell, 80-100 mesh) was from Beijing Guanghua Timber Mill. Dimethyl sulfoxide (DMSO), acetone, tetrahydrofuran and dichloromethane were obtained from Tianjin Kermel Chemical Reagent Development Center, China. All the reagents were analytical grade unless otherwise specified and used as received.

2. Characterization

The powder X-ray diffraction (PXRD) patterns were obtained using Rigaku D/Max 3400 powder diffractometer with Cu Kα radiation (λ = 0.15418 nm). Fourier transform infrared (FT-IR) spectra were collected on a Bruker Tensor 27 FT-IR spectrometer in KBr media. The nuclear magnetic resonance spectra of ^{13}C with cross-polarization magic-angle spinning (^{13}C CP/MAS NMR) were taken on a Bruker DRX-400 spectrometer at 100.5 MHz with a spinning frequency of 8 kHz. The thermogravimetric analysis (TGA) measurements were carried out under N_2 flow on a NETZSCH STA 409 PC instrument. Samples were heated at a heating rate of 10 ^oC/min from 35 to 800 ^oC in an N_2 flow of 30 mL/min. N_2 physical adsorption–desorption measurement was carried out at 77 K on an Autosorb-1 Quantachrome instrument. Samples were pre-degassed at 150 °C to remove water and other physically adsorbed species. The specific surface areas for N_2 were calculated using the Brunauer-Emmet-Teller (BET) model in the range of $0.05 < P/P_o < 0.35$. The pore size distributions were calculated from the adsorption isotherms by nonlocal density functional theory (NLDFT), slit pore, equilibrium model. Microstructures of the materials were examined by transmission electron microscopy (TEM, JEOL JEM-2000EX). Morphology of the samples was observed by field-emission scanning electron microscopy (SEM, FEI Quanta 200F). The vapor-phase adsorption of benzene experiment was performed at 273 K on a Micromeritics ASAP 2020 system. Prior to the measurement, the samples were degassed at 120 °C for at least 5 h.

3. Preparation of FOFs

1.5 mmol of DFF dissolved in 5 mL of DMSO was added into 25 mL two necked flasks equipped with a magnetic stir bar and a water-cooled reflux condenser. The reactor was degassed using three evacuation-N_2-backfill cycles. Then appropriate amount of amine monomer (1:1 ratio of aldehyde to amine functional group) dissolved in 1.5 mL DMSO was slowly injected into the reactor

over 10 min at 50 ^{o}C under nitrogen atmosphere. After stirring at 50 ^{o}C for 20 min, the oil bath was heated to 180 ^{o}C and the reaction mixture was further refluxed under nitrogen atmosphere for 24 h. The obtained crude product was evacuated and washed with 100 mL of acetone, tetrahydrofuran and dichloromethane for 2 h, respectively.

4. TGA curves

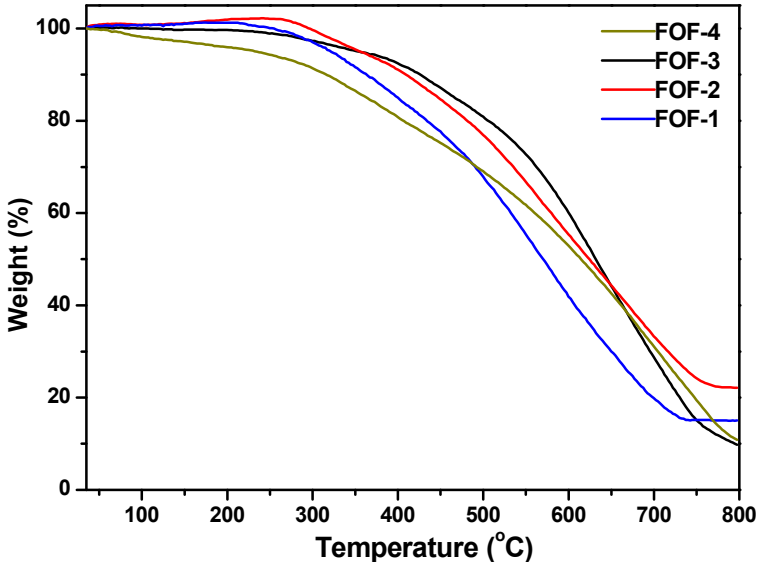

Fig. S1. TGA traces of FOFs.

5. FT-IR spectra of FOF material with corresponding feedstock materials

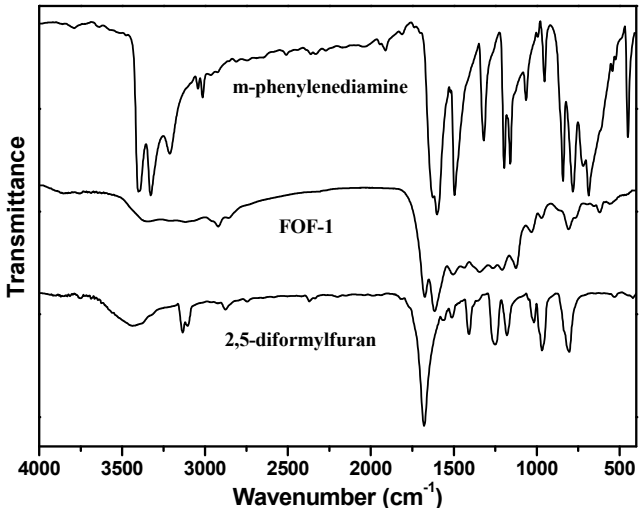

Fig. S2. FT-IR spectrua of *m*-phenylenediamine, FOF-1 and 2,5-diformylfuran.

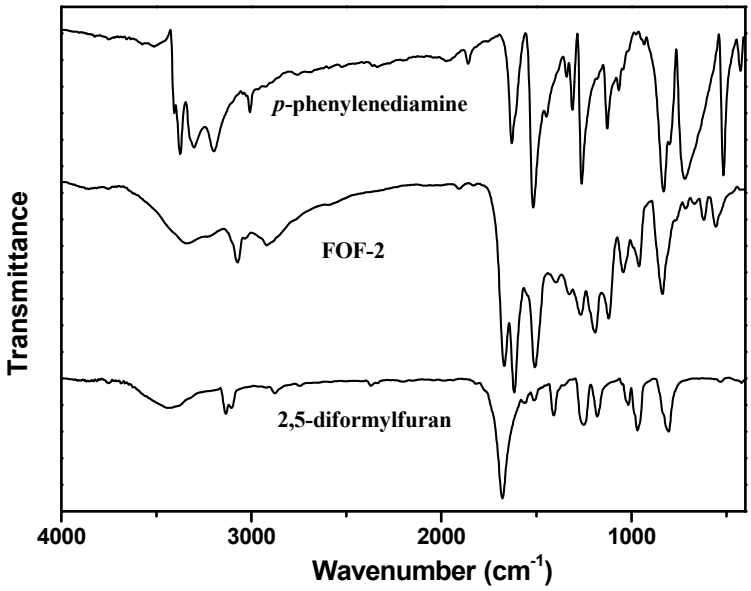

Fig. S3. FT-IR spectrua of *p*-phenylenediamine, FOF-2 and 2,5-diformylfuran..

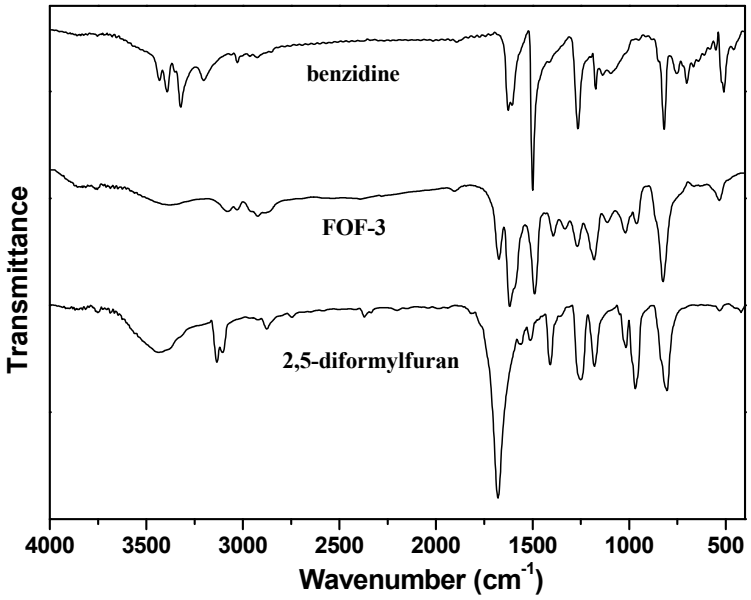

Fig. S4. FT-IR spectra of benzidine, FOF-3 and 2,5-diformylfuran..

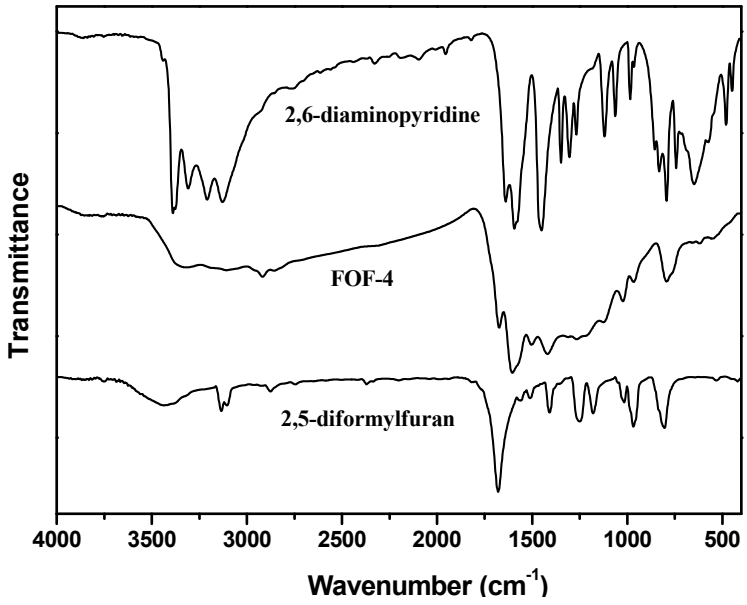

Fig. S5. FT-IR spectra of 2,6-diaminopyridine, FOF-4 and 2,5-diformylfuran.

6. XRD patterns

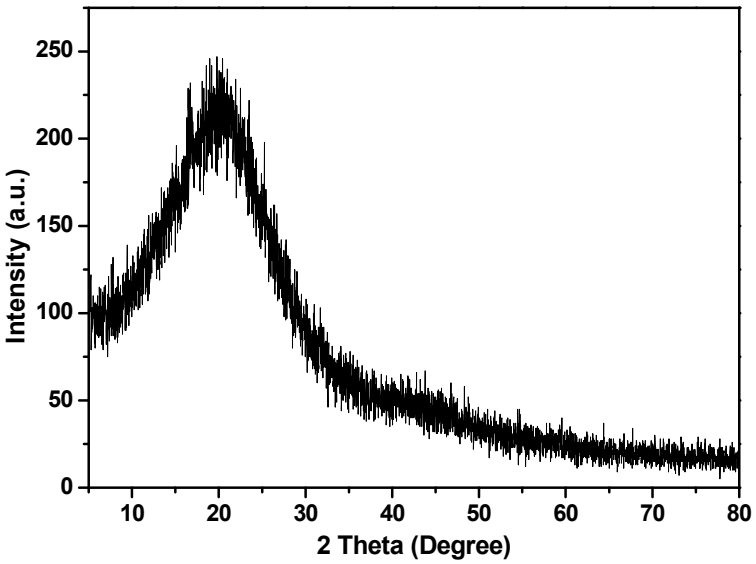

Fig. S6. PXRD pattern for FOF-1.

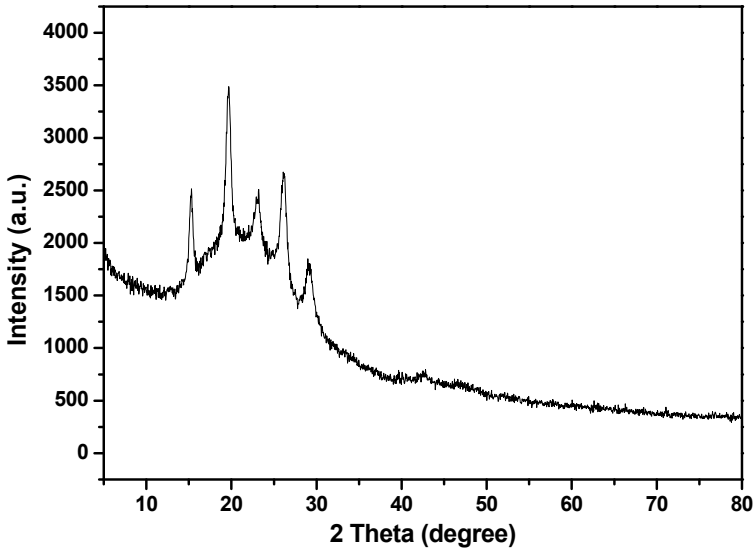

Fig. S7. PXRD pattern for FOF-2.

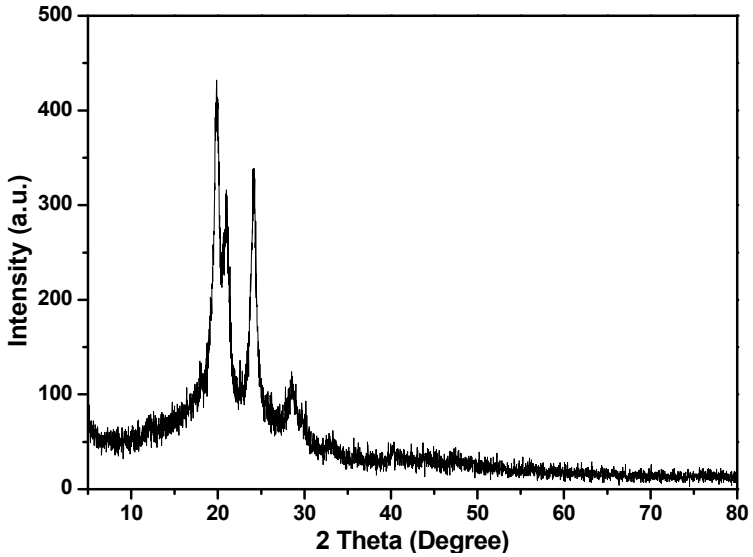

Fig. S8. PXRD pattern for FOF-3.

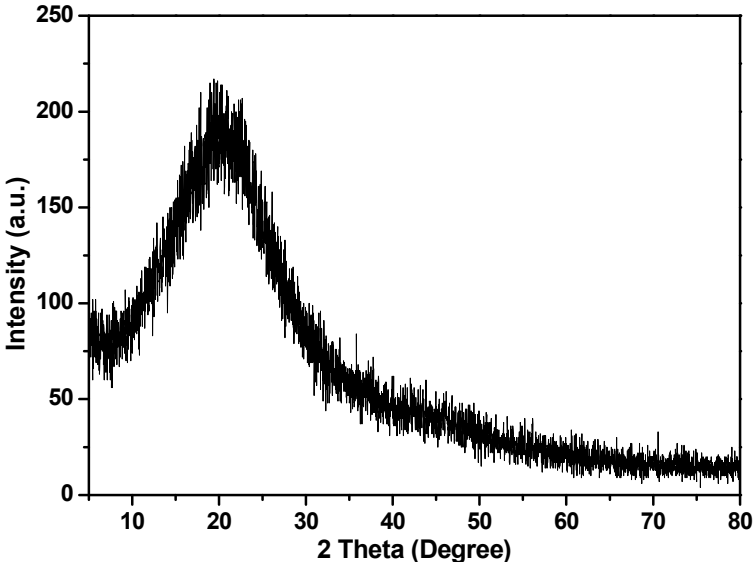

Fig. S9. PXRD pattern for FOF-4.

7. BET plots of FOFs

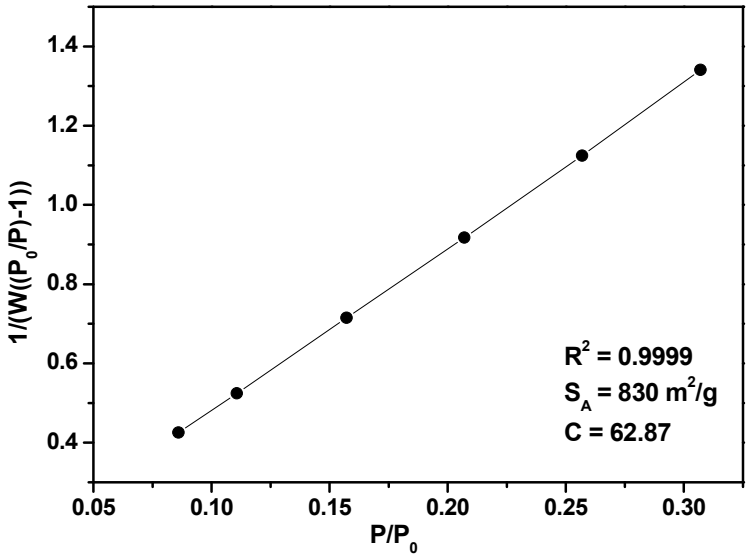

Fig. S10. BET plot for FOF-1 calculated from N_2 adsorption data.

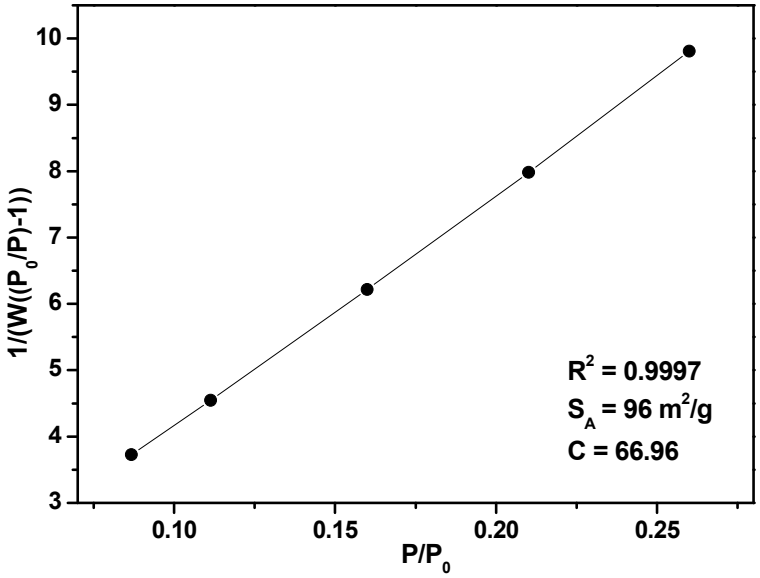

Fig. S11. BET plot for FOF-2 calculated from N_2 adsorption data.

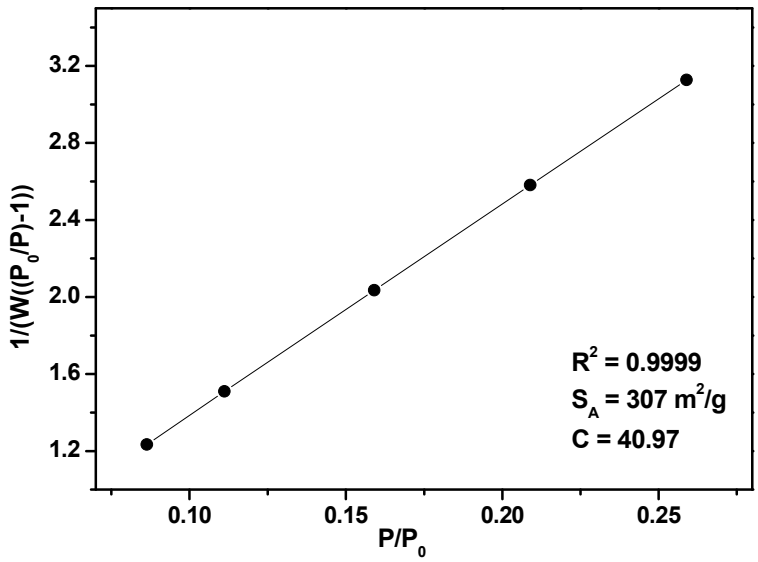

Fig. S12. BET plot for FOF-3 calculated from N_2 adsorption data.

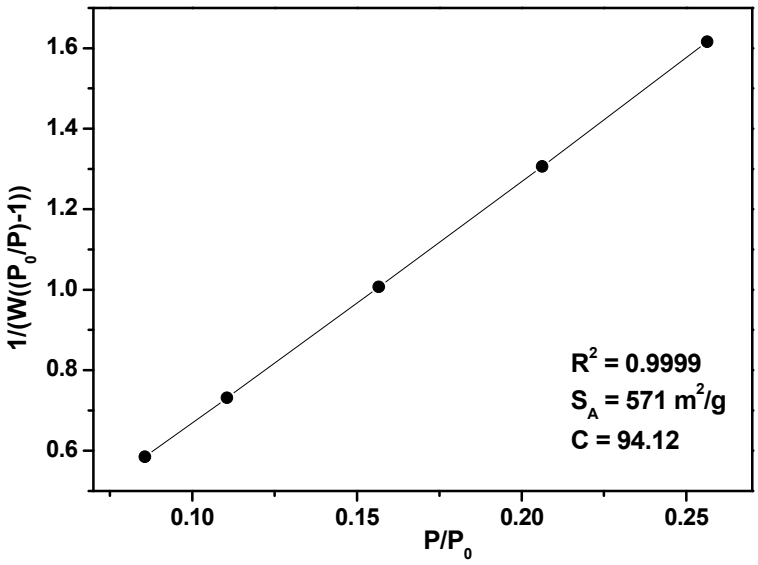

Fig. S13. BET plot for FOF-4 calculated from N_2 adsorption data.

8. Pore size distribution

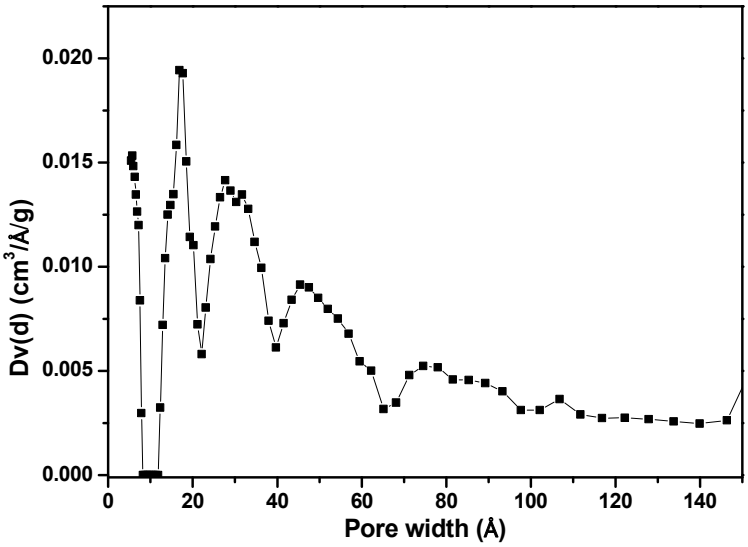

Fig. S14. Pore size distribution histogram of FOF-1 calculated by NLDFT method.

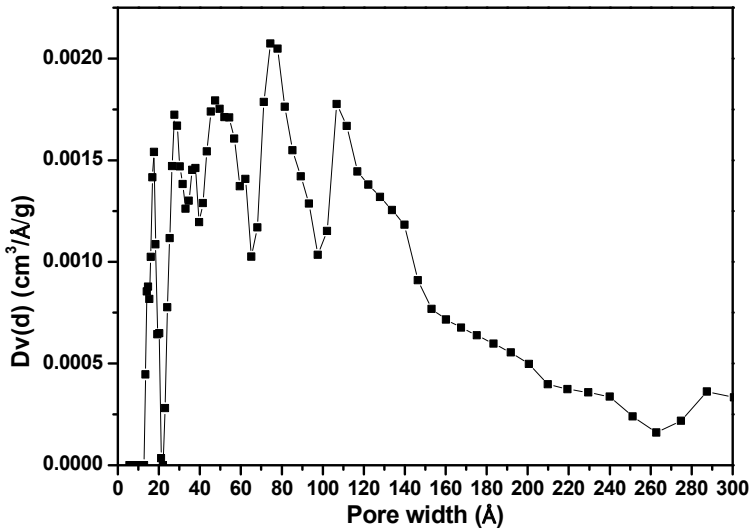

Fig. S15. Pore size distribution histogram of FOF-2 calculated by NLDFT method.

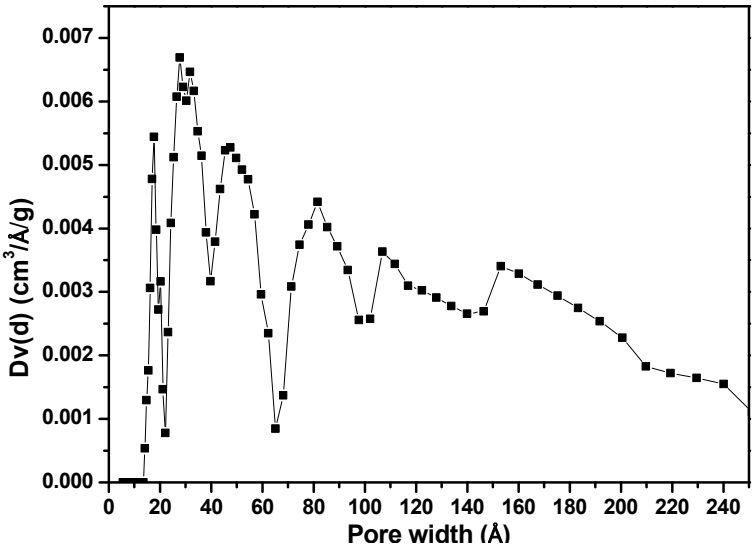

Fig. S16. Pore size distribution histogram of FOF-3 calculated by NLDFT method.

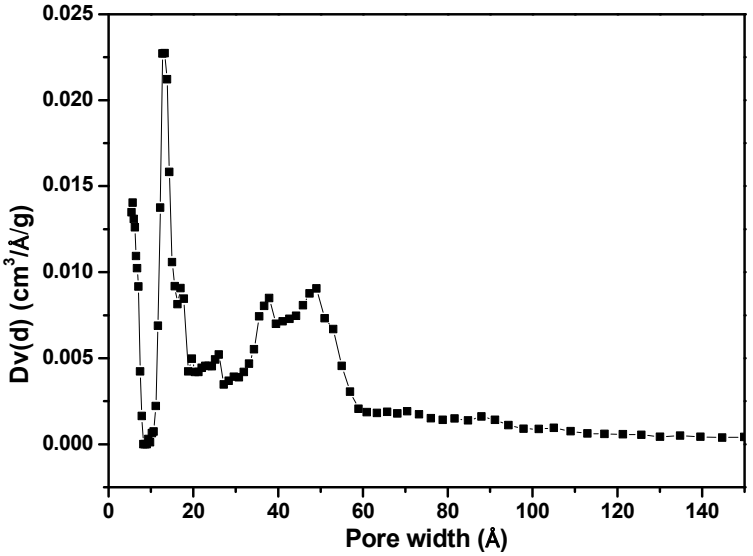

Fig. S17. Pore size distribution histogram of FOF-4 calculated by NLDFT method.